Acta Cryst. (1998). D**54**, 473–475

Crystallographic studies of casein kinase I δ: toward a structural understanding of auto-inhibition

KENTON L. LONGENECKER, PETER J. ROACH AND THOMAS D. HURLEY* *at Department of Biochemistry and Molecular Biology, Indiana University School of Medicine, Indianapolis, IN 46202, USA. E-mail: hurley@biochem4.iupui.edu*

(*Received 21 April 1997; accepted 2 September 1997*)

Abstract

A recombinant form of mammalian casein kinase I δ (CKIδ) containing the catalytic domain and an auto-inhibitory domain was expressed in *Escherichia coli*, purified and crystallized. X-ray data were collected to 2.4 Å resolution, and the crystals belong to space group $C222_1$. Molecular replacement using the structure of the catalytic domain of CKIδ yielded strong electron density for residues in the model, but no interpretable density was found for the inhibitory domain. A conserved intermolecular contact suggests the formation of dimers which would inhibit the activity of this protein kinase.

1. Introduction

As a protein kinase, casein kinase I (CKI) is a member of the large family of phosphotransferases involved in cell-regulatory processes. CKI activity is found in all eukaryotes and the enzyme phosphorylates multiple protein substrates, suggesting that it is involved in a variety of important cellular functions (Tuazon & Traugh, 1991). CKI has an unusual preference for phosphorylating substrates that are already phosphorylated. An important recognition motif for CKI activity is a phosphorylated serine or threonine located three residues N-terminal to the amino acid targeted for phosphorylation (Flotow *et al.*, 1990).

Recombinant cDNA cloning reveals a family of CKI enzymes (Rowles *et al.*, 1991) containing similar catalytic domains of about 300 amino acids and C-terminal extensions that vary in length and sequence. CKIδ is a mammalian isoform that is most closely related to homologs involved in the regulation of DNA repair in yeast (Graves *et al.*, 1993). Recently, we determined the crystal structure of CKI$\delta\Delta$317, an active truncation mutant of CKIδ lacking residues C-terminal to 317 (Longenecker *et al.*, 1996). An anion binding site identified on the surface of CKIδ probably corresponds to the binding site for the phosphate ester of the substrate recognition motif. This recognition mechanism presumably extends to other family members as it is consistent with the structure of the catalytic domain of Cki1 (Xu *et al.*, 1995). Cki1 is a CKI homolog from *Schizosaccharomyces pombe* that shares 56% sequence identity with CKIδ over the catalytic domain. An interesting feature of CKIδ is the involvement of phosphorylation in the regulation of its enzymatic activity. The analysis of C-terminal truncation mutants identified an auto-inhibitory domain between residues 317 and 342 in CKIδ (Graves & Roach, 1995). Truncation at residue 342 is the minimal construct that displays the wild-type auto-inhibitory properties. Inhibition is due to autophosphorylation of residues in this regulatory region, and activation is observed upon dephosphorylation with the type I protein phosphatase. Phosphorylated residues in the auto-inhibitory domain may cause it to be a pseudo-substrate, competing with substrate binding (Graves & Roach, 1995; Longenecker *et al.*, 1996). Seeking to understand the structural basis for this auto-inhibition, we pursued further crystallographic studies of CKIδ truncated at residue 342 so as to include the auto-inhibitory domain.

2. Experimental procedures

A plasmid encoding the truncation mutant CKI$\delta\Delta$342 (Graves & Roach, 1995) was modified by polymerase-chain-reaction mutagenesis to encode H6CKI$\delta\Delta$342 in which the sequence MAHHHHHHA is added at the N-terminus. Extracts from transformed *E. coli* cells were prepared and enzyme activity was measured as described elsewhere (Graves & Roach, 1995; Longenecker *et al.*, 1996). Crude homogenate was adsorbed to 2–3 ml Ni^{2+}-NTA-agarose (Qiagen, Chatsworth, CA) and loaded in a column. The column was washed with 50 m*M* Tris–HCl, pH 8.0, 0.5 *M* NaCl and 10 m*M* imidazole, and bound protein was eluted with 50 m*M* Tris–HCl, pH 8.0, 0.2 *M* NaCl and 100 m*M* imidazole. The eluate was diluted tenfold in cold buffer containing 50 m*M* sodium citrate, pH 6.0, and 1 m*M* dithiothreitol, and applied to a 9 ml SP–sepharose column equilibrated with buffer *A* (50 m*M* sodium citrate, pH 6.0, 1 m*M* dithiothreitol and 5 m*M* β-octyl glucoside). Protein was eluted by a 240 ml linear gradient of 10–60% buffer *B* (50 m*M* sodium citrate, pH 6.0, 1 m*M* dithiothreitol and 1 *M* NaCl) in buffer *A*. Protein was dialyzed against 60 m*M* Tris–HCl, pH 7.5, 1 m*M* dithiothreitol and 5 m*M* β-octyl glucoside, and concentrated to 8 to 10 mg ml^{-1}. The inclusion of β-octyl glucoside in the protein solution was necessary to insure a monodispersed solution. Crystals were grown by vapor diffusion using a sitting drop, combining equal volumes of concentrated protein and reservoir solution (18–22% PEG MME 2000, 0.2–0.3 *M* ammonium sulfate, 1 m*M* manganese chloride and 50 m*M* sodium citrate, pH 5.3) and also by microseeding. X-ray diffraction data were generated using a Rigaku RU-200-HB rotating-copper-anode generator and collected at room temperature on a RAXIS IIC image-plate detector. Data were processed with *BIOTEX* software (Molecular Structure Corporation, 1995). The apparent molecular mass of H6CKI$\delta\Delta$342 was analyzed by gel filtration chromatography using a Superose 12 column (Pharmacia) equilibrated with 50 m*M* sodium citrate, pH 6.0, 0.1 *M* NaCl and 1 m*M* dithiothreitol.

3. Results and discussion

Cation exchange chromatography of H6CKI$\delta\Delta$342 using SP–sepharose separated four peaks of activity. Column fractions were combined for each peak separately, yielding pools *A*, *B*, *C* and *D* labeled according to their order of elution. A typical purification from 6 l of culture yielded 1.0 mg protein in pool *A*, 1.5 mg in pool *B*, 4.5 mg in pool *C*, and 3.6 mg in pool *D*.

These pools likely reflect multiple phosphorylation states as observed in studies of Cki1 and cAPK (Carmel *et al.*, 1994; Herberg *et al.*, 1993). Each of the samples can be activated by type I protein phosphatase treatment, concomitantly increasing their mobility on SDS–PAGE. The samples appear highly purified by SDS–PAGE analysis, but isoelectric focusing reveals multiple bands for all of the samples. Despite the heterogeneity, plate-like crystals were grown of pool *B* and *C* protein. X-ray data were collected and both crystals were found to be orthorhombic $C222_1$ (Table 1). Data were also processed as the primitive lattice setting, but no evidence for pseudo-centering of a primitive lattice was found. A V_m of

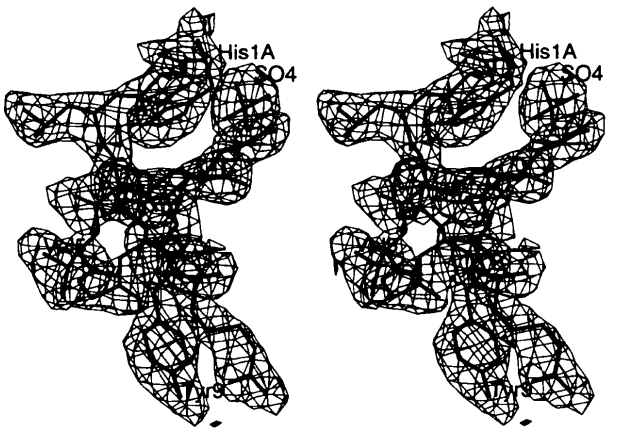

Fig. 1. Stereo diagram of the electron density for the N-terminus of the H6CKIδΔ342 structure. Partial refinement yielded this $2F_o - F_c$ map contoured at 1 standard deviation with electron density for an alanine, a histidine (His1A) and a sulfate anion (SO_4) which were not in the molecular-replacement search model. Val5 and Tyr9 (CKIδ numbering) are also labeled.

Table 1. *Data-collection statistics for H6CKIδΔ342 crystals*

	Pool *B* Native	Pool *B* + PCMBS	Pool *C* Native	Pool *C* + PCMBS
a (Å)	80.7	80.3	80.4	80.5
b (Å)	102.5	101.8	102.0	102.1
c (Å)	94.7	93.9	94.0	94.2
$\alpha = \beta = \gamma$ (°)	90	90	90	90
Maximum resolution (Å)	2.50	2.66	2.40	2.66
Observations	33583	22521	43532	23710
Unique reflections	12249	8965	13682	9648
Completeness (top shell) (%)	88 (63)	79 (60)	88 (53)	84 (56)
Total $I/\sigma(I)$	11.1	8.9	13.2	5.1
R_{merge} (%)	8.9	9.9	6.6	11.9
R_{iso} (%)		22		27

2.38 Å^3 Da^{-1} suggested one 40 kDa molecule in the asymmetric unit (Matthews, 1968).

A molecular-replacement solution was calculated with the program *AMoRe* (Collaborative Computational Project, Number 4, 1994; Navaza, 1994) using the structure of CKIδΔ317, which consists of residues 1–216 and 224–293 (PDB code 1CKI, Longenecker *et al.*, 1996), as the search model. For pool *C* data, the top solution for the rotation function was 3.4 standard deviations higher than the next highest peak, and a translational position was found which yielded an *R* factor of 0.38. The packing arrangement of the molecules in the unit cell for this solution yielded no unfavorable intermolecular contacts. Electron-density maps calculated with these molecular-replacement models yielded strong density for much of the model, but very little density for residues not contained in the model. Partial refinement yielded a model containing residues 1–216 and 221–293 that had an *R* value of 0.24 and a free *R* value of 0.33 for data between 8 and 2.70 Å (Brünger, 1992). Electron density

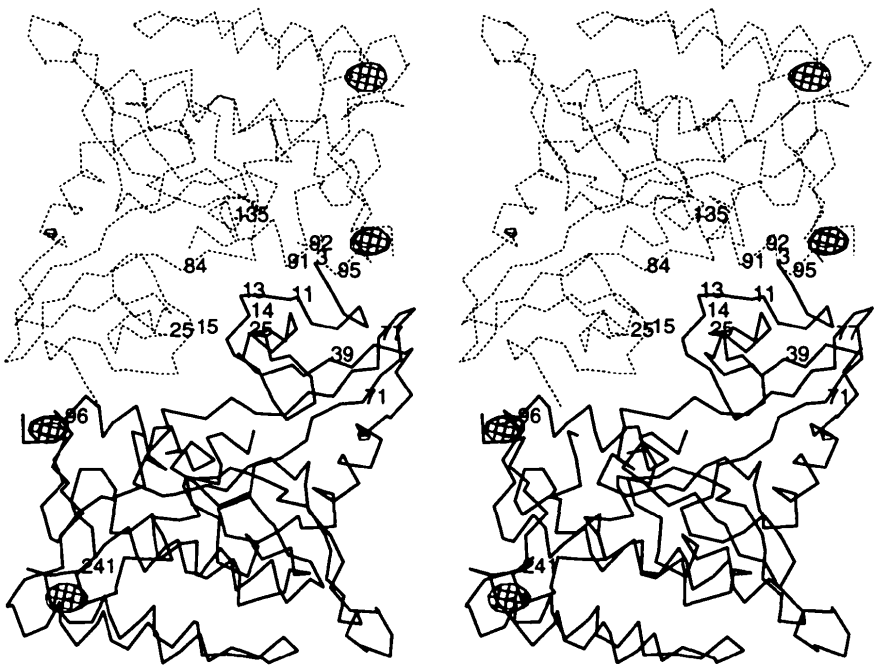

Fig. 2. Molecular-replacement solution and difference Fourier for a PCMBS derivative of H6CKIδΔ342. This stereo diagram shows the Cα trace for the one molecule of the asymmetric unit (thick lines) and a symmetry-related molecule (dashed lines). Difference electron density for a PCMBS derivative is contoured at 5 standard deviations (thin lines), revealing major sites of modification by Cys96 and Cys241, and a minor site by Cys71. Amino acids apparently important in forming this dimer include Leu3, Leu11, Arg13, Lys14, Leu25, Leu39 and Tyr77 from one monomer, and Ile15, Leu25, Leu84, Asp91, Leu92, Phe95 and Leu135 from the other monomer (CKIδ numbering). Note that only half of the interactions are labeled in the figure.

improved for certain portions, including one of the six histidines on the N-terminus, but not for residues on the C-terminus (Fig. 1). Calculations with data from pool *B* crystals yielded similar results.

The lack of density for residues of the auto-inhibitory domain may arise from disorder, poor phases from the model or proteolysis during crystallization. Proteolysis was ruled out by SDS analysis on protein obtained from crystals (data not shown). In order to minimize phase bias from a starting model missing nearly 18% of the residues contained in the crystallized protein, Fourier coefficients from the model were weighted using the program *SIGMAA* (Collaborative Computational Project, Number 4, 1994; Read, 1986). *SIGMAA* estimated the root-mean-square coordinate error to be 0.62 Å and calculated an overall mean figure of merit of 0.64 for the resolution range 6.0 to 2.5 Å. Additional phase information was obtained from heavy-atom-derivative data collected on crystals soaked with 50 μ*M* *p*-chloro-mercuri benzene sulfonate (PCMBS) for 5 d (Table 1). Peaks on both difference Patterson and difference Fourier maps (Fig. 2) were easily interpreted. Various phase sets were calculated using *XTALVIEW* (McRee, 1993) and *PHASES* (Furey & Swaminathan, 1990) and combined with molecular-replacement phases using *SIGMAA*. For example, a 2.8 Å SIR phase set ($R_{\text{Cullis}} = 0.64$) was combined with the model phases to yield a phase set with a figure of merit that improved to 0.72. However, the resulting electron-density maps yielded no additional structural information for the auto-inhibitory domain, so it appears to be disordered in both crystal forms. Given the heterogeneity in the crystallized samples, the disorder may be due to multiple discrete conformations and/or phosphorylation states of the auto-inhibitory domain.

The molecular-replacement solution highlights a potentially important intermolecular contact. Crystals of CKIδΔ317 belong to space group $P2_12_12_1$ and contain two molecules in the asymmetric unit (Longenecker *et al.*, 1996) The interaction between the two molecules across the non-crystallographic twofold axis in these crystals is essentially the same interaction observed across one of the crystallographic twofold axes in H6CKIδΔ342 crystals (Fig. 2). This result suggests that CKIδ crystallizes as dimers, but whether CKIδ forms a dimer *in vivo* is unknown. Gel-filtration analysis suggests H6CKIδΔ342 is monomeric in solution (data not shown). Although additional evidence concerning dimerization has not been obtained, the extensive and conserved nature of this interaction is intriguing. The buried molecular surface area for a monomer upon dimerization is 1566 Å^2, a value typical for biologically relevant protein–protein interactions (Janin & Chothia, 1990). The structures suggest that dimerization could be an additional mechanism for inhibiting the enzyme. In both crystal forms, Arg13 inserts into the adenine binding pocket of the symmetry-related molecule of the dimer, and would prevent ATP binding and perhaps the binding of large substrates.

Several mechanisms for activation and inhibition of protein kinases have been elucidated through crystallographic studies (Johnson *et al.*, 1996). Two examples of protein kinases with auto-inhibitory domains that are contiguous with the catalytic domain like CKIδ are twitchin kinase and the calmodulin-dependent protein kinase I. Crystal structures of these two protein kinases show multiple specific contacts between the auto-inhibitory domain and the catalytic domain that prevent proper conformation of the enzyme for catalysis and also inhibit substrate binding (Hu *et al.*, 1994; Goldberg *et al.*, 1996). For CKIδ, binding of a phosphorylated residue from the auto-inhibitory domain to the anion binding site in the catalytic domain could interfere with substrate binding. Dimerization of CKIδ would provide an additional mechanism for inhibition. While dimerization is a well established mechanism for activation of certain protein tyrosine kinases (Ullrich & Schlessinger, 1990), formation of homodimers has not been identified as a mechanism for inhibition of protein kinases. Whether such regulation of CKIδ occurs *in vivo* remains to be established.

Further studies will be necessary to establish the structural basis for auto-inhibition of CKIδ by phosphorylation. Several serine and threonine residues in the inhibitory domain can be phosphorylated resulting in multiple isomers which can crystallize in the same lattice. Structural ambiguity of the auto-inhibitory domain suggests that inhibition can be achieved *via* multiple conformations of the inhibitory domain which reduce enzymatic activity by competitive binding of any one of the phosphorylated residues to the phosphate-recognition site in the catalytic domain. Future studies will focus on reducing the heterogeneity within the protein sample by further purification or removal of phosphorylation sites by mutagenesis.

References

Brünger, A. T. (1992). *X-PLOR, Version 3.1, A System for X-ray Crystallography and NMR*. Yale University, New Haven, Connecticut, USA.

Carmel, G., Leichus, B., Cheng, X., Patterson, S. D., Mirza, U., Chait, B. T. & Kuret, J. (1994). *J. Biol. Chem.* **269**, 7304–7309.

Collaborative Computational Project, Number 4 (1994). *Acta Cryst.* D**50**, 760–763.

Flotow, H., Graves, P. R., Wang, A., Fiol, C. J., Roeske, R. W. & Roach, P. J. (1990). *J. Biol. Chem.* **265**, 14264–14269.

Furey, W. & Swaminathan, S. (1990). *Am. Crystallogr. Assoc. Meeting Suppl.* **18**, 73.

Goldberg, J., Nairn, A. C. & Kuriyan, J. (1996). *Cell*, **84**, 875–887.

Graves, P. R., Haas, D. W., Hagedorn, C. H., DePaoli-Roach, A. A. & Roach, P. J. (1993). *J. Biol. Chem.* **268**, 6394–6401.

Graves, P. R. & Roach, P. J. (1995). *J. Biol. Chem.* **270**, 21689–21694.

Herberg, F. W., Bell, S. M. & Taylor, S. S. (1993). *Protein Eng.* **6**, 771–777.

Hu, S., Parker, M. W., Lei, J. Y., Wilce, M. C. J., Benian, G. M. & Kemp, B. E. (1994). *Nature (London)*, **369**, 581–584.

Janin, J. & Chothia, C. (1990). *J. Biol. Chem.* **265**, 16027–16030.

Johnson, L. N., Noble, M. E. M. & Owen, D. J. (1996). *Cell*, **85**, 149–158.

Longenecker, K. L., Roach, P. J. & Hurley, T. D. (1996). *J. Mol. Biol.* **257**, 618–631.

McRee, D. E. (1993). *Practical Protein Crystallography*. San Diego: Academic Press.

Matthews, B. W. (1968). *J. Mol. Biol.* **33**, 491–497.

Molecular Structure Corporation (1995). *BIOTEX*. MSC, 3200 Research Forest Drive, The Woodlands, TX 77381, USA.

Navaza, J. (1994). *Acta Cryst.* A**50**, 157–163.

Read, R. J. (1986). *Acta Cryst.* A**42**, 140–149.

Rowles, J., Slaughter, C., Moomaw, C., Hsu, J. & Cobb, M. H. (1991). *Proc. Natl Acad. Sci. USA*, **88**, 9548–9552.

Tuazon, P. T. & Traugh, J. A. (1991). *Adv. Second Messenger Phosphoprotein Res.* **23**, 123–164.

Ullrich, A. & Schlessinger, J. (1990). *Cell*, **61**, 203–212.

Xu, R., Carmel, G., Sweet, R. M., Kuret, J. & Cheng, X. (1995). *EMBO J.* **14**, 1015–1023.